Progress in Oceanography 168 (2018) 1–12

Contents lists available at ScienceDirect

Progress in Oceanography

journal homepage: www.elsevier.com/locate/pocean

Spatial variability and size structure of particles and plankton in the Fram Strait

E. Trudnowska[a,b,*], S. Sagan[a], K. Błachowiak-Samołyk[a]

[a] Institute of Oceanology Polish Academy of Sciences, Poland
[b] Centre for Polar Studies KNOW (Leading National Research Centre), Poland

A B S T R A C T

Changes within marine pelagic fields in the Arctic affect global biogeochemical cycles. The size structure and distribution of particles and plankton (P&P) were studied in the main northward passage of Atlantic water to the Arctic region, which is affected in various ways by climate change. The wide size spectrum of P&P (3 µm–5 mm) was assessed by combining measurements from two complementary optical counters, a Laser In-Situ Scattering and Transmissometry (LISST) instrument and a Laser Optical Plankton Counter (LOPC). The measurements were performed in the upper 100 m layer at 55 stations in summer in 2013. The P&P were attributed to various functional groups – particles, phytoplankton, marine snow, and zooplankton – to test their spatial coupling with hydrodynamic forcing. Although our study confirms that the Fram Strait is a region of strong biophysical contrasts, the expected coastal-offshore gradient has not been distinguished clearly. Three mechanisms could explain P&P patches: particle flocculation due to contact with fresh waters from ice and fjords, enhanced production due to coastal upwelling as well as widening the range of warm surface water advection northwards. Particularly rich biological hot spots were recognised in the northern, shallow parts of the west Spitsbergen shelf, and near the marginal ice edges, confirming that these areas are highly vulnerable to marine predators. Moreover, combining optical measurements from two size-specific optical counters contributes greatly to reducing the substantial knowledge gap regarding wide size structure and distribution of thus far neglected seawater components, such as non-living particles and marine snow aggregates, occurring in this vulnerable Arctic region.

1. Introduction

The transport of water volume, heat, and salt to the Arctic Ocean drives global thermohaline circulation and thus, influences the Earth's climate. Changes within marine pelagic fields in the Arctic affect global biogeochemical cycles (Worden et al. 2015; Carmack et al., 2016); therefore, there is an urgent need to improve understanding of the environmental patterns, ecological relationships, and various processes occurring within Arctic marine systems in this era of rapid climate change. In the European Arctic, the Fram Strait is a key area for heat and organic matter exchange between the North Atlantic and the Arctic Ocean. The northward penetration of warm Atlantic water (AW) into the Arctic Ocean not only affects its thermal conditions and sea ice cover, but also determines the amount and structure of primary and secondary producers. The two main currents in the Fram Strait are the East Greenland Current (EGC), carrying cold Arctic waters southward, and the West Spitsbergen Current (WSC), bringing relatively warm AW northward. Interactions between these two currents, together with fjord water exchange, results in strong mesoscale variability (Piechura et al., 2001; Schauer et al., 2004; Beszczynska-Möller et al., 2012). In addition, heterogeneous topography and the presence of both baroclinic and barotropic eddies contribute to substantial mixing and recirculation within the Fram Strait (Schlichtholz and Houssais, 2002; Wekerle et al., 2017). The EGC and WSC differ not only in their hydrography but also in their optical properties (Cisek et al., 2010; Granskog et al., 2015; Pavlov et al., 2015). This complex physical environment results in highly variable primary production in space and time (Cherkasheva et al., 2014).

Hop et al. (2007), in their review of the biological characteristics of the pelagic system across the Fram Strait, stated that until 2007 the main phytoplankton bloom was dominated by diatoms. In recent years, the amount of dinoflagellates and flagellates has increased and blooms of *Phaeocystis pouchetii* now occur frequently (Bauerfeind et al., 2009; Saiz et al., 2013; Nöthig et al., 2015). Zooplankton is dominated by copepods (*Calanus* spp. and *Oithona* spp.) and is concentrated mainly in the uppermost 100 m during summer (Blachowiak-Samolyk et al., 2007; Carstensen et al., 2012; Gluchowska et al., 2017). The 'atlantification' of the Fram Strait, in the case of zooplankton, has been observed mainly in the form of northern shifts in the latitudinal extensions of warm-water boreal species (Kraft et al., 2012; Bauerfeind et al., 2014; Weydmann et al., 2014). Although a number of investigations have already been conducted, considerable uncertainty still exists about the scale of the advection of particles and plankton (P&P) through the Fram Strait (Basedow et al., 2018).

One of the most relevant indicators of ecosystem functionality and energy fluxes is P&P size structure (Richardson and Schoeman, 2004;

* Corresponding author at: Institute of Oceanology Polish Academy of Sciences, Poland.
E-mail address: emilia@iopan.pl (E. Trudnowska).

https://doi.org/10.1016/j.pocean.2018.09.005
Received 21 July 2017; Received in revised form 30 August 2018; Accepted 10 September 2018
Available online 11 September 2018
0079-6611/

Lane et al., 2008), which has not altogether been studied in the European Arctic. As P&P span several orders of magnitude in size, it is very difficult to comprehensively measure their composition and size structure. Previous studies of P&P used mainly traditional sampling equipment (sediment traps, bottles, and nets) and produced rather fragmented information on their selected fractions, including living organisms (bacteria, protists, zooplankton), detritus, and mineral particles (e.g. Wassmann et al., 2006; Pasternak et al., 2008; Bauerfeind et al., 2009; Nöthig et al., 2015).

The need to investigate interactions between physical and biological processes in the pelagic realm has stimulated new, holistic methodological approaches. To account for the great temporal and spatial variability in P&P distributions, as well as to simultaneously measure their quantity and size structure with environmental variables, various automatic optical techniques have been developed and applied (Serra et al., 2003; Wiebe and Benfield 2003; Herman et al., 2004). These can provide high resolution, ataxonomic, size-based P&P measurements (Sprules and Barth 2015). Because most important ecological and physiological processes scale with size, this approach may be at least as useful, if not more, as standard taxonomic studies for gaining insight into the structure and functioning of pelagic communities (Kerr and Dickie 2001; Jennings et al., 2002; Krupica et al., 2012). Size-specific plankton functional types are an important denominator incorporated into global biochemical models to better quantify interactions between ocean ecosystems and the climate cycle (Quéré et al., 2005).

This is the first study to analyse the fundamental property of the Arctic marine system: the wide size spectrum of P&P (3 μm – 5 000 μm) together with their functional composition and distribution. The objective of this study was to identify coastal-offshore gradient in the volume and size structure of various P&P types in the Fram Strait region. Ultimately, analysing P&P distribution and size structure with a combination of two complementary optical counters enabled us to demonstrate that spatial coupling exists between hydrodynamic forcing and particles, phytoplankton, marine snow, and zooplankton, in an area of the Arctic that is crucial for marine predators.

2. Materials

2.1. Data collection

Measurements of the biophysical environment and distributions of P&P were conducted in summer in 2013 (13–22 July) on board the RV *Oceania*. Measurements were performed both during 'day' (28 stations) and 'night' (27 stations) hours. Because no statistical differences in the vertical distribution of size fractions (Kolmogorov-Smirnov test, $p > 0.05$) were observed, daily cycles were not taken into consideration during further analyses. The study area was the eastern Fram Strait and an adjacent region north of Svalbard. Sampling was performed at 55 stations located along seven sections (Fig. 1). Vertical profiles of the environmental measurements and P&P distributions were obtained in the upper 100 m by a range of instruments, all mounted on the same platform. These were: a Laser In-Situ Scattering and Transmissometry instrument (LISST-100X, type B, Sequoia Scientific, Inc., WA, USA), a Laser Optical Plankton Counter (LOPC, Brooke Ocean Technology Dartmouth, Canada), a conductivity-temperature-depth sensor system (CTD, SBE 911plus, Seabird Electronics Inc., USA), and a fluorometer (Seapoint Sensors Inc., USA). The water column of the upper 100 m was chosen because it is the zone of the main primary production, with the highest accumulation of mesozooplankton biomass and the strongest light attenuation by sinking organic material. To achieve the best possible quality and consistency, data from the upper 2 m were discarded; this minimises false counts due to wave action, stray light, or air bubble formation. The data were averaged over 1 and 10 m depth intervals. All data were processed using Matlab software (Mathworks, USA). Hydrography and P&P distribution maps were prepared with Ocean Data View Software (Schlitzer, 2015). Statistical tests were performed in Statistica 10 (StatSoft) and PRIMER 7/PERMANOVA+.

2.2. Instrumentation

The LISST-100X, type B, measures the volume concentration of particles of 1–250 μm with a 6 mm thick laser beam travelling the optical path of 5 cm through the water. Particle sizes are inferred from the laser diffraction method, relying on measurements of the volume scattering function at near-forward angles that are interpreted on the basis of Mie theory, under the general assumption that particles are spherical, to obtain the particle size distribution (Agrawal and Pottsmith, 2000). Since at the diffraction limit scattering is weakly dependent on the refraction index, it is not possible to directly distinguish organic and mineral particles (Karp-Boss and Boss, 2007). Commonly observed non-spherical particles can affect the obtained size distributions through an apparent increase in the presence of small particles due to optical scattering from the subscales of larger particles (Graham et al., 2012). Despite these limitations, the utility of LISST for accessing nano- and microplankton (Angles et al., 2008), as well as phototrophic bacteria (Serra et al., 2003), has been validated by calibration studies with simultaneous microscopic counts. Simultaneous fluorescence measurements allow the presence of phytoplankton cells to be assessed. Scattering by deionised water was chosen as the background reference.

The LOPC is an optical *in situ* sensor that autonomously counts and measures all particles passing its beam path in the sampling tunnel (7 × 7 cm wide). The portion of light blocked by the particle is measured and recorded as a digital size, which is converted to equivalent spherical diameter (*ESD*) using a semi-empirical formula based on calibration with dark spheres of known diameters (Herman 1992; Herman et al., 2004). The technical specifications allow for counting and size-fractioning of particles in the size range of 100–35,000 μm *ESD*. Abundance and size distribution data were used to calculate the particles' volume according to the spherical model.

The CTD and fluorometer were connected directly to the LOPC to provide simultaneous data on environmental conditions and as a proxy of algae concentration, respectively.

2.3. Spatial variability and size structure of P&P

The main source of AW inflow to the Arctic is divided into branches and partly recirculates southward (Walczowski, 2013). Our aim was to study how the core of the WSC differs from the Recirculating Atlantic Current (REC); shelf slope (SS); and northern Svalbard region (NS), where the WSC bifurcates into Yermark and Svalbard branches. Accordingly, the data were grouped into sub-regions based on hydrographic measurements from the water column (data not shown, Beszczynska-Möller personal communication) and existing literature (Saloranta and Haugan, 2004; Beszczynska-Möller et al., 2012).

To vertically partition the water column by diverse P&P types and their mean size, analysis was conducted at 10 m averaged depth intervals. To identify variation within sub-regions, confidence intervals (± 0.95) were plotted with mean values.

The P&P size structure was analysed using normalised volume spectrum (*nVd*), which is a convenient way of displaying particle volume distribution over a large size range without losing the relationship between the area under the curve, when plotted as a function of log(*d*), and the integrated particle volume (Jackson & Checkley, 2011). The equation for *nVd* is as follows:

$$nVd = \frac{\Delta N}{\Delta d} \cdot \frac{\pi}{6} d^4$$

where ΔN is the abundance of P&P within a size interval, Δd is the linear size interval, and d is the diameter of P&P in a size class. *nVd* is unitless and expressed as parts per million (ppm). To identify variation within sub-regions, mean values were plotted with standard errors and

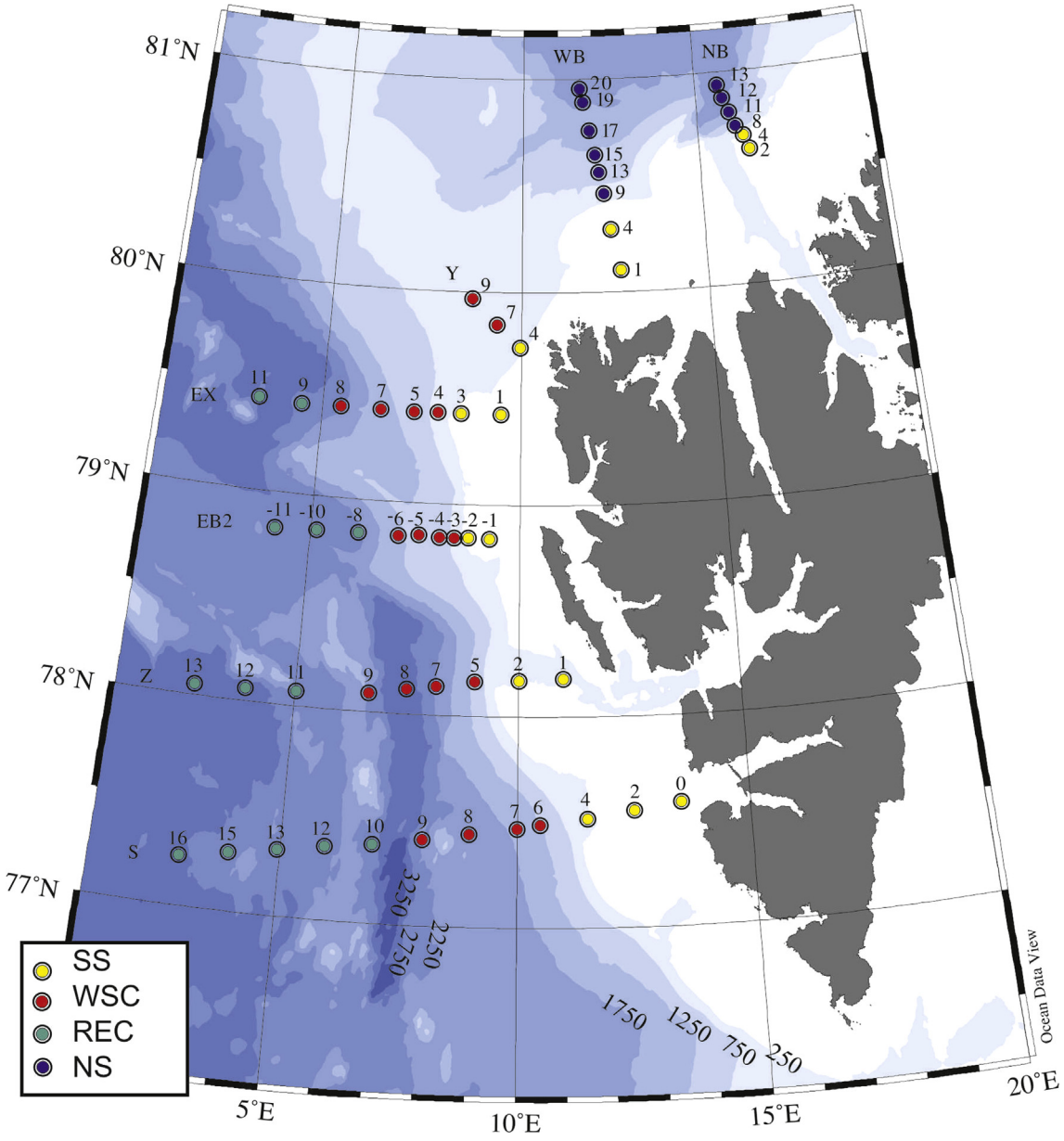

Fig. 1. Map of the sampling stations in the eastern Fram Strait. Various hydrographical regimes related to different regions (SS: shelf-slop, WSC: West Spitsbergen Current, REC: Recirculating Atlantic Current, NS: northern Svalbard) are indicated by particular colours.

median values with 25% and 75% percentiles.

2.4. Particle type classification

To avoid potential errors at the lower and upper ends of the instruments' limitations (Stemmann et al., 2008), we restricted data to 3–100 μm for the LISST (21 size classes) and to 100–5000 μm for the LOPC (34 size classes). The upper size limits were designated to eliminate the 'unexpected case effect' caused by under-sampled size classes (Blanco et al., 1994; Stemmann et al., 2008), as well as to avoid contamination from signals due to the presence of large particles outside the upper size limit of the LISST (Mikkelsen et al., 2005; Davies et al., 2012). The smallest size classes from the LISST (< 3.2 μm) were excluded, as these are highly sensitive to deviations caused by stray light (Reynolds et al., 2010; Andrews et al., 2011).

To test how various size fractions of LISST measurements were associated with primary production (phytoplankton cells), we analysed the relationship between the particle volume of each size class and chlorophyll fluorescence at 10 m depth intervals. This correlation was performed for each sub-region. All LISST data were differentiated by the coefficient of determination (R^2), which determines the proportion of variance 'explained' by the regression model (Nagelkerke, 1991). In practice, we used the R^2 value of each correlation as a measure to predict the proportion of phyto-type particles and assigned the remaining part to the other particle type (Fig. 2).

The best currently known method for distinguishing between zooplankton and snow-type particles in LOPC concerns only relatively large particles that occlude more than two laser elements: Multi Element Plankton (MEP) particles (Jackson and Checkley, 2011). However, since MEP particles generally constitute < 2% of all particles assessed by the LOPC (Espinasse et al., 2017), we decided to modify an original method of Jackson and Checkley (2011) to incorporate the Single Element Plankton (SEP) particles that fulfil the same principle, i.e. the relationship between the particle's spherical diameter (d) and occluded diameter (OD, the number of laser elements that particle is intercepting) (Fig. 2, Supplementary Fig. 1). We tested this method against

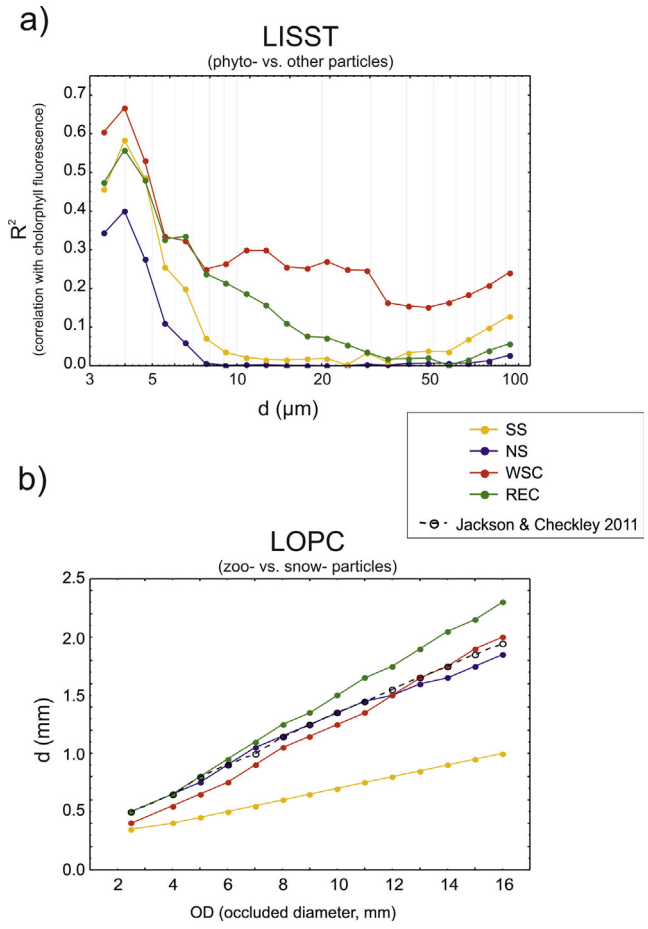

Fig. 2. The rules of differentiation of the particle types. (a) The LISST data were differentiated on the basis of the correlation between the particles biovolume within each size class and the chlorophyll fluorescence, according to the definition of the coefficient of determination (R^2), which determines the proportion of variance explained by the regression model (Nagelkerke, 1991), which was directly used as a measure of predicting the part of phyto-type particles (the area under the curve) and other-type particles (the area above the curve). (b) The LOPC counts were differentiated according to the relationship between the particle spherical diameter (d) and the occluded diameter (the number of laser elements that particle is intercepting, OD) (Supplementary material Fig. 1). In general, snow-particles intercept a lot of laser elements, but do not reach high overall size (the area below the fitting curve), while the zooplankton does not intercept a lot of laser elements regardless of its size (the area above the fitting curve). This method was originally developed by Jackson and Checkley (2011), but in this paper we modified it to use also the SEP particles (see method section). Each fitting presents the combined datasets for each particular sub-region (SS: shelf-slop, WSC: West Spitsbergen Current, REC: Recirculating Atlantic Current, NS: northern Svalbard).

zooplankton abundance data estimated by net sampling: 12 samples that were collected in 2013 concurrently with the measurements of this study and 17 zooplankton samples collected in 2012 in the same area (published in Trudnowska et al., 2016; Gluchowska et al., 2017). We obtained a satisfactory correlation between LOPC counts of zooplankton type particles and net estimated zooplankton abundance ($R^2 = 0.87$) (Supplementary Fig. 2) after excluding six outliers for which LOPC counts were extremely high in comparison to net zooplankton abundance.

We utilised a few additional existing methods for better LOPC data interpretation. The first one estimates aggregate contribution to the overall P&P volume by fitting a log-normal distribution to the *nVd* spectrum (Petrik et al., 2013; Jackson et al., 2015). The second method analyses particle transparency (AI index), which is defined as the ratio between mean digital size (DS) of middle laser diodes and maximum DS (Table 1). It was developed to distinguish between relatively opaque copepods and more transparent particles (Checkley et al., 2008) and was successfully tested in the north Atlantic Ocean (Basedow et al., 2013). The last method, which analyses the percentage of MEP particles (%MEP) in total LOPC counts, was developed to emphasise the high contribution of detritus, when %MEP > 2 (Espinasse et al., 2017).

Table 1
. The parameters describing the aggregate signal in P&P dataset. The volume spectrum (*nVd*, ppm) of aggregates, the percent of the aggregate volume (% aggregate) to total P&P volume, the number of laser elements that particle is intercepting (OD), the attenuance index (AI, a proxy for transparency) and the percent of Multi Element Plankton (%MEP) in total LOPC counts. Each column presents the mean of combined datasets for each particular sub-region (SS: shelf-slop, WSC: West Spitsbergen Current, REC: Recirculating Atlantic Current, NS: northern Svalbard).

Parameter/Region	SS	NS	WSC	REC
nVd of aggregates (ppm)	4.7	6.7	4.2	4.1
% aggregates	43.9	52.8	60.1	59.3
OD	4.30	4.13	3.85	3.91
AI	0.131	0.097	0.098	0.123
% MEP	1.1	1.9	1.4	1.5

3. Results

3.1. Types and size structure of the P&P

The volume of each P&P size fraction derived via the LISST correlated significantly with chlorophyll fluorescence, particularly for the small size fractions ($p < 0.001$, for particles 3–6, 3–8, and 3–18 µm in the NS, SS, and REC regions, respectively; Fig. 2a). The WSC region had the highest overall correlation, and the correlation was statistically significant across the entire investigated size spectrum (3–100 µm). The contribution of the phyto-type particles was in general relatively high at open sea locations (WSC and REC stations), whereas at the shelf and northernmost locations (NS and SS stations), the other-type particles clearly dominated (Fig. 2a).

The distinction between marine snow and zooplankton type particles was derived from LOPC measurements, based on analysing the relationship between estimated diameter (*d*) and occluded diameter (*OD*). Our results were in general very similar to the relationship originally described by Jackson and Checkley (2011), presented as a black line on Fig. 2b), with a slightly higher contribution of large marine snow at the REC stations. A very different fit was obtained in the shelf region (SS), which indicates the small diameter size and large *OD* typical of the amorphous structure of marine snow. However, a third type of P&P (in between snow- and zoo-type) could potentially reduce the ability of this method to make a distinction between types in the SS region (Supplementary Fig. 1).

The results of the fitting procedure to the *nVd* spectra indicate that the highest volume of aggregates was at the NS stations, although aggregates were estimated to contribute more to overall P&P volume at the WSC and REC stations (Table 1). On average, the P&P occluded more laser elements (higher *OD*) at the NS and SS stations and were rather amorphous and transparent at the NS and WSC stations (low AI index). The percent of MEPs in total P&P counts was highest at the NS stations and lowest in the SS region (Table 1).

The size structure of P&P accessed via LISST was generally characterised by a peak in phyto-type particles in the smallest size fractions (up to 10 µm), but at the WSC locations the phyto-type particles were also observed within larger size fractions (Fig. 3, Supplementary Fig. 3). The peak of other-type particles was shifted towards a little bit larger size fractions. An especially large volume of large other-type particles was observed in the NS region, which agreed also with high volume of

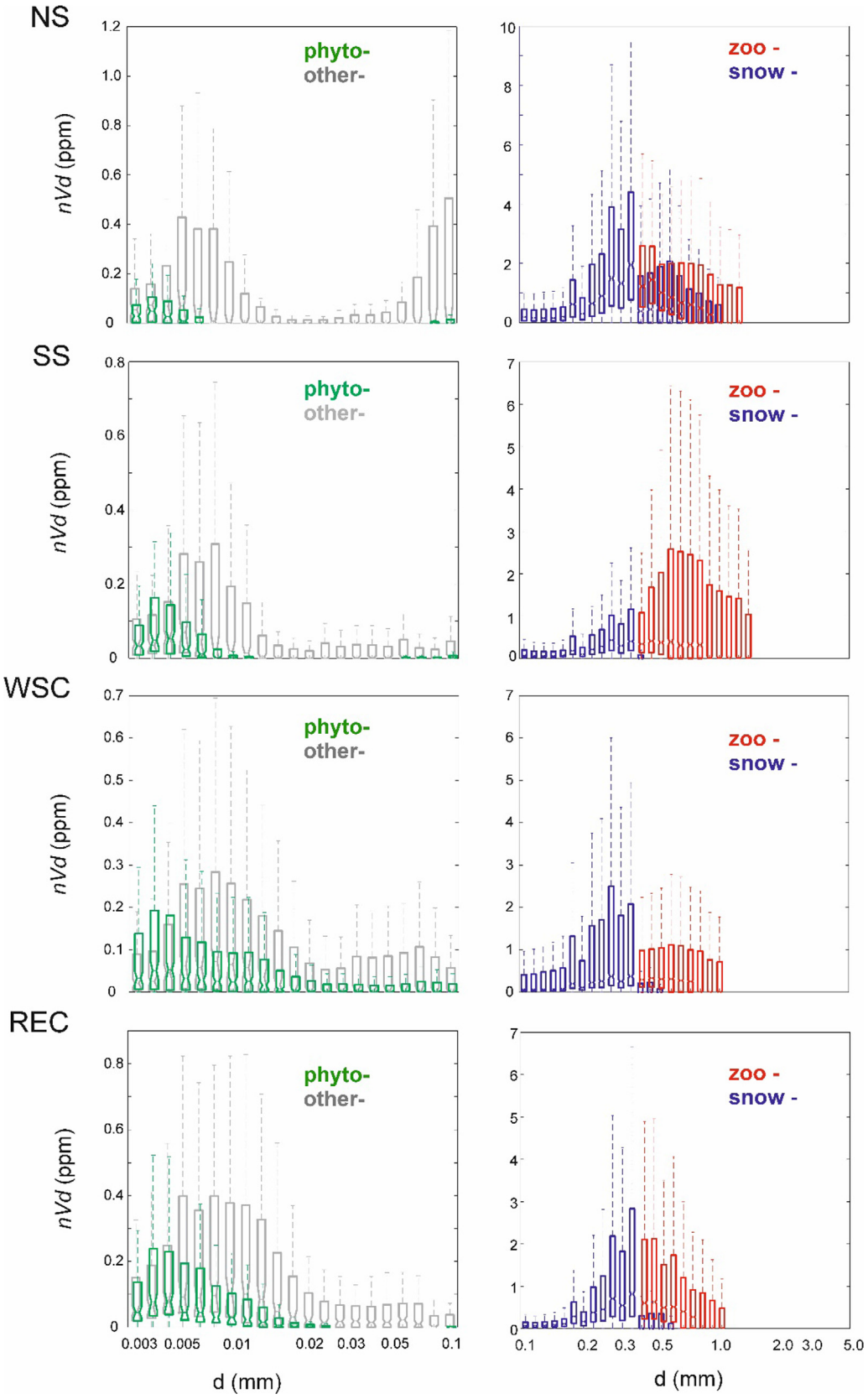

Fig. 3. The medians with 25 and 75% quartiles of volume size spectra (*nVd*) of the phyto- and other- types of particles measured by the LISST (left side) and zoo- and snow- type of particles measured by the LOPC (right side). Each graph presents the combined datasets for each particular sub-region (SS: shelf-slope, WSC: West Spitsbergen Current, REC: Recirculating Atlantic Current, NS: northern Svalbard).

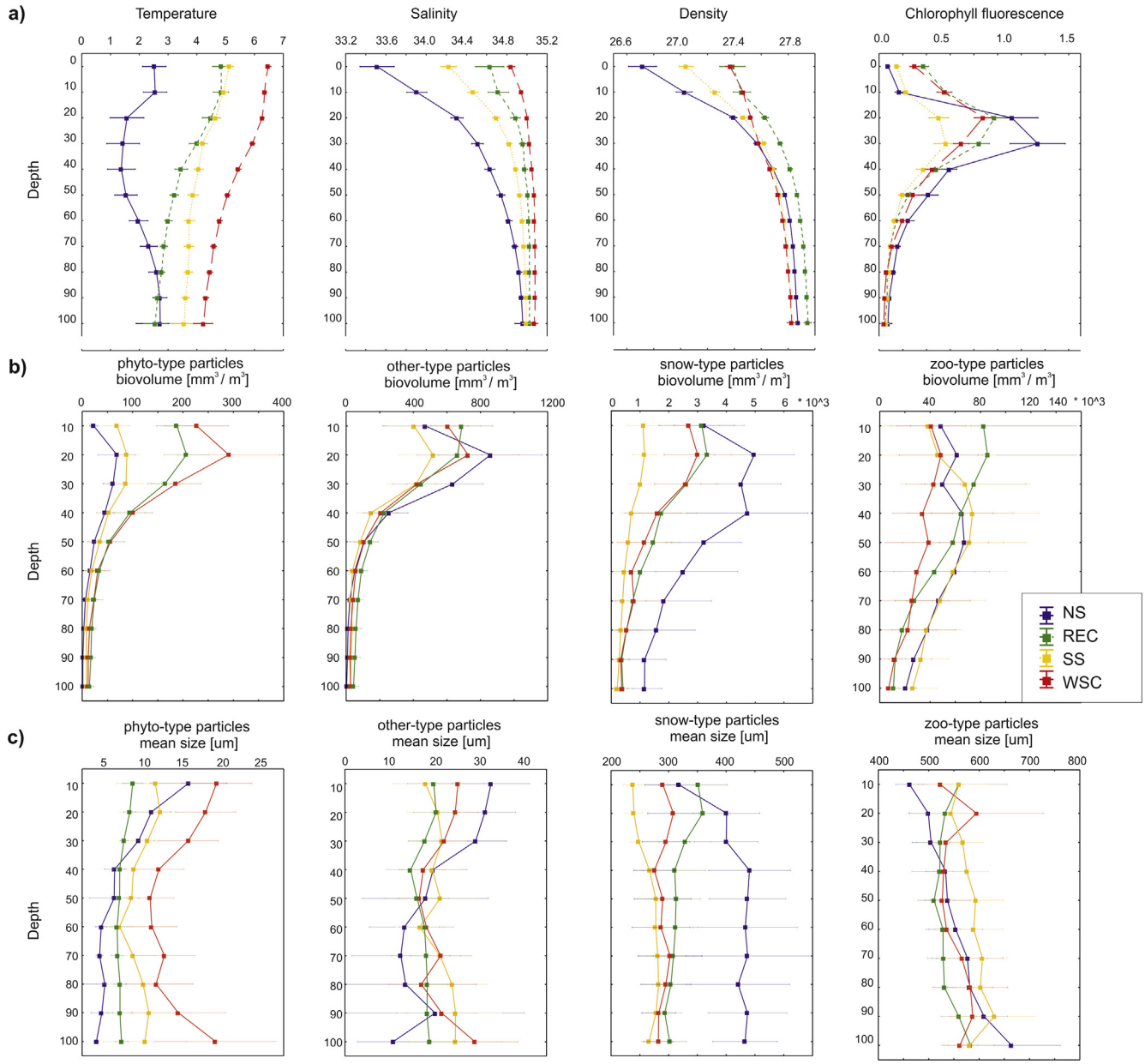

Fig. 4. The vertical profiles of 10-m mean (± 0.95 confidence interval) temperature, salinity, density, chlorophyll fluorescence (first row) and the biovolume (mm^3/m^3) and mean size (d, μm) of various types of particles (phyto-, other-, snow- and zoo-) within specified sub-regions (SS: shelf-slope, WSC: West Spitsbergen Current, REC: Recirculating Atlantic Current, NS: northern Svalbard).

and snow-type particles in the LOPC results. The size structure of snow-type particles was similar among other regions (peak at ~ 300 μm), with the lowest total volume content observed in the SS region. The volume of zooplankton was high, but also varied greatly in SS locations. It was also dominated by rather smaller fractions, the same as at the REC stations (Fig. 3; Supplementary Fig. 3).

3.2. Vertical gradients by region

A typical summer pattern of vertical hydrographical stratification was observed, i.e. fresher, lighter, and slightly warmer water in the upper 20 m layer with more stable conditions underneath (Fig. 4a). The peak of chlorophyll fluorescence was generally observed to be around 20–30 m depth and was the highest in the NS region. The small particles derived from LISST were concentrated mainly within the upper 40 m (Fig. 4b). The volume of phyto-type particles was the highest at the WSC and REC stations; the volume of the other particles was very similar among all regions, with a slightly higher volume at the NS stations. The NS region was characterised by the highest volume and largest size (Fig. 4b, c) of marine snow-type particles, which were concentrated mainly within the upper 50 m. The lowest amount and smallest size of marine snow-type particles was observed at the SS stations. The distribution of zooplankton-type particles was characterised by very high variability, but on average it was rather similar among regions and depth layers, both in terms of volume and size (Fig. 4b, c).

3.3. Horizontal coupling between hydrodynamic forcing and P&P distribution

The study region was characterised by high spatial variability in the studied parameters (Fig. 5). The average seawater temperature was highest in the WSC region (5.33 °C) and lower at stations located in the other sub-regions (4.14 °C at the SS, 3.57 °C at the REC, and 2.06 °C at

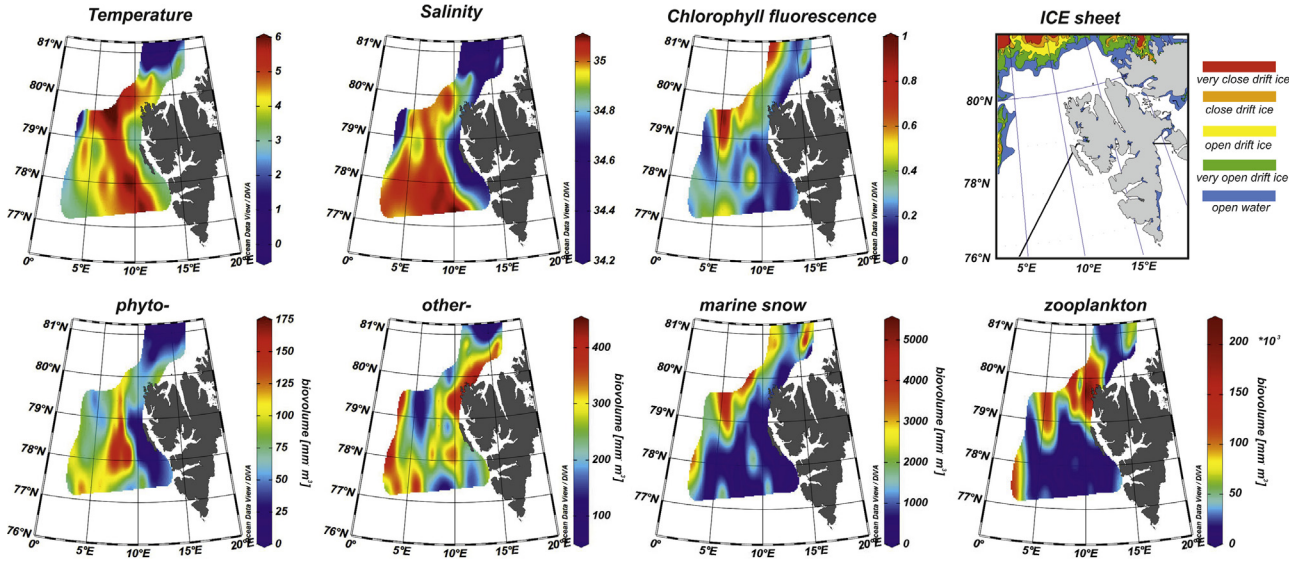

Fig. 5. 1st row: the horizontal distribution of temperature, salinity and chlorophyll fluorescence at stations (upper 100 m) in the eastern Fram Strait together with the ice cover (data source: Norwegian Meteorological Institute). 2nd row: the horizontal distribution of phyto-, other-, snow- and zoo-type particles biovolume (mm^3/m^3) at investigated stations (upper 100 m).

the NS stations). The average salinity across the studied 100 m layer was lower in the NS (34.5) and SS (34.8) regions compared to the WSC and REC regions (35.0 and 34.9, respectively). A peak of chlorophyll fluorescence was observed in the northern open water parts of the study area (northern edges of each region), while the lowest values of chlorophyll fluorescence were recorded at the coastal and shelf stations. During sampling, we were very close to the ice sheet at the northern edges of the NS region and at the western edges of the EX and EB sections (Fig. 5).

The phyto-type particles were mainly concentrated at the WSC stations, whereas other small particles concentrated at the northern SS, NS, and most offshore stations in the REC region, relatively close to the ice edge (Fig. 5). The peaks of marine snow volume distribution corresponded highly with the locations of highest chlorophyll fluorescence. Zooplankton was concentrated in the northern end of the WSC, the primary site of water advection to the study area.

P&P volume composition structure did not differ significantly among the defined hydrographical regions (ANOSIM test, $R < 0.25$, Fig. 6). The NS group was the only region that varied slightly from the others, mainly due to the high volume of marine snow and other-types of particles in relation to phyto-type particles. When plotting the volume distribution of various P&P types, their main concentrations fell on the left side of the nMDS plot. The geographic location of these study stations is indicated by pink dots on the map subplot (left side of Fig. 6). This distribution corresponded well with the edges of the ice sheet and the shallow north end of Atlantic Water advection.

4. Discussion

4.1. Methodological issues

The original idea of this study was to merge results from two independent optical particle counters to build a joint spectrum of the entire P&P size range. However, the size spectra observed by the LOPC and LISST agreed mainly in shape, but not in terms of P&P volume and abundance: the LOPC indicated higher concentrations than the LISST (this can clearly be seen at the border of the spectra, as a discrepancy between upper size limit of the LISST and lower size limit of the LOPC, but also as the higher intercepts of LOPC spectra), so we could not obtain a smooth transition between those two approaches (Supplementary Fig. 4). This discrepancy in obtained volumes and numbers of P&P can partially be explained by the smaller volume sampled by the LISST compared to the LOPC. A further explanation is that each technique uses a different physical property to measure the size and density of P&P: the LISST uses light scattering, whereas LOPC detection is based on light absorption. And this difference is especially important in the case of marine snow aggregates, because their interaction with incident light vary greatly due to their porosity; non-spherical shape and internal structure; thus, the relationship between their diameters and volumes gets complicated and may lead to discrepancies between results of the two different optical methods applied (Jackson et al., 1997; Jackson and Checkley, 2011; Karp-Boss and Boss, 2007; Stemmann et al., 2008; Graham et al., 2012). Other attempts to merge data from different instrument types encountered similar problems (Jackson et al., 1997; Mikkelsen et al., 2005; Stemmann et al., 2008). Therefore, we ultimately decided to consider the datasets from the two instruments separately.

Even if neither the LISST nor the LOPC can distinguish between living plankton, detritus, and other non-living suspensions, it is possible to interpret some of the P&P volume distribution data through dedicated data processing and basing on existing general knowledge about seawater content. The LISST measurements were divided into phyto- and other-type particles by applying the coefficients obtained from the correlations with simultaneous chlorophyll fluorescence measurements (Fig. 2). We are aware that this is a simplified approach, which may incorporate to some extent other than chlorophyll absorbing pigments, such as phaeopigments associated with particles other than living phytoplankton, that can be important in coastal waters (Babin et al., 2003). Therefore, we regard the phyto-group as being of organic origin (not only active primary producers) and the other-type group as being composed of mainly mineral and/or other non-living particles. The high correlation between chlorophyll fluorescence and P&P volume indicated that an important fraction of P&P observed in our study was either phytoplankton cells and colonies or pigment-rich faecal pellets and aggregates. However, the reliability of this approach was questionable at the NS stations, where the correlations were the weakest, most probably because of their locality close to marginal sea ice zone, which resulted in a complicated, difficult to interpret mixture of P&P.

Other previous attempts to analyse the size spectra derived from different instruments indicated the high importance of non-living P&P in the water column, which was nevertheless underestimated before using optical devices (Jackson et al., 1997; Mikkelsen et al., 2005;

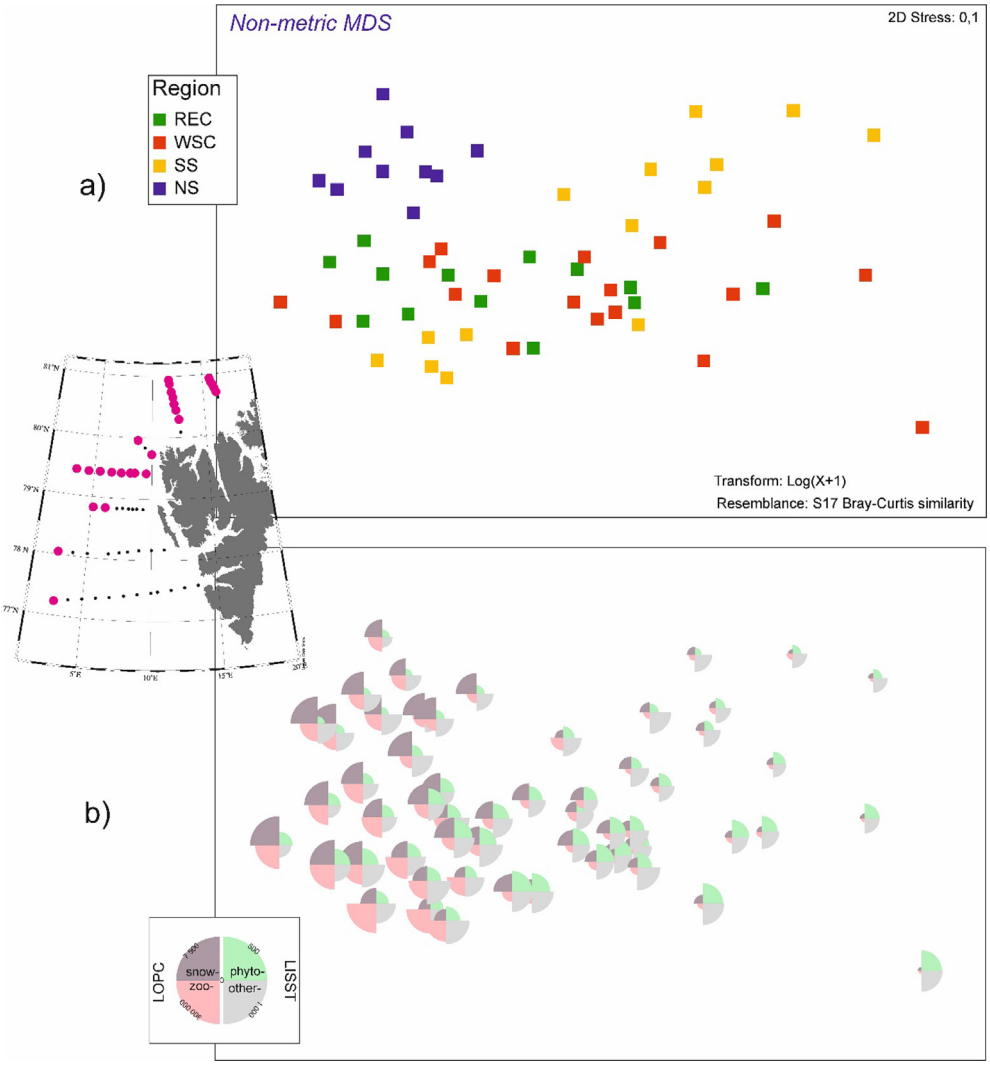

Fig. 6. The multidimensional scaling of the composition of various types of particles (phyto-, other-, snow-, zoo-) at particular stations indicated by region (a) SS: shelf-slope, WSC: West Spitsbergen Current, REC: Recirculating Atlantic Current, NS: northern Svalbard; and by the volume of particular P&P types (b). The pink dots on the map indicate the geographical location of plankton hotspots (left side of the MDS plot).

Stemmann et al., 2008). To qualitatively interpret the LOPC data, we applied a set of currently available methods (*ESD-OD* relationship: Jackson and Checkley, 2011, aggregate fitting to *nVd*: Petrik et al., 2013; %MEP: Espinasse et al., 2017). Additionally, we successfully tested the first method, i.e. the pattern of relationships between the estimated (*ESD*) and occluded (*OD*) diameter of P&P with traditional net sampling (Supplementary Fig. 2). The *ESD-OD* in most sub-regions was very similar to previously observed relationships (Jackson et al., 2011; Petrik et al., 2013; Trudnowska et al., 2014), with the exception of the SS region, where a third mode of P&P was observed in-between marine snow and zooplankton (Fig. 2, Supplementary Fig. 1). In total particle counts, the percentage of MEPs was close to 2%, which is a threshold above which the LOPC is most likely counting more detritus than living organisms (Espinasse et al., 2017). This points towards the high importance of marine snow and aggregates in total P&P counts, especially at the NS stations, and generally agrees with their high percentage in total volume and high primary production levels in this region (Table 1). The major difference between zooplankton net and LOPC results is observed in areas with detritus products from large phytoplankton blooms (Vandromme et al., 2014).

Our study showed that aggregates constituted 22–77% of total P&P volume within the upper 100 m layer of the Fram Strait region in summer 2013. This procedure of fitting aggregate-volume to the LOPC size spectra was previously verified by extensive simultaneous net sampling in the continental shelf of the Bay of Biscay (Vandromme et al., 2014), with the conclusion that LOPC measurements are sufficient to estimate zooplankton volume and size structure, provided that data is adequately processed. Thus far, only very few studies attempted to distinguish between zooplankton and non-living particles. The results of these studies are striking: of the total P&P in the seawater, zooplankton accounted only for 0.1–15% in the Mediterranean Sea (Stemmann et al., 2008) or approximately 20% in the California Current (Gonzalez-Quiros and Checkley, 2006; Jackson and Checkley, 2011). The contribution of living zooplankton to total particles varied greatly with size fraction (smaller at smaller size classes), but also among shelf (0–25%), slope (2–48%) and main basin (10–55%) in the Beaufort Sea (Forest et al., 2012). We also observed the size- and region-related variation in the relations between phyto-others and zoo-snow particles (Fig. 3). The substantial importance of material other than zooplankton (e.g. small mineral particles in glacial bays, marine aggregates) in the overall plankton density and biomass was recorded also in the Svalbard fjords (Trudnowska et al., 2012, 2014). *In situ* holographic camera observations indicated that the majority of suspended matter does not exist as isolated particles, but is bound up in larger flocculated particles (Graham et al., 2012). Generally, the aggregation process affects phytoplankton cells, mineral particles,

zooplankton faecal pellets, organisms' body fragments, detritus, and other marine snow objects. Therefore, those flocculated particles are, by definition, composed of multiple sub-components and play a major role in trophic interactions, both pelagic and pelago-benthic zone. However, this role is still underestimated because the marine snow aggregates are so fragile that they can only be observed *in situ*.

Despite some obvious limitations and uncertainties, by using two *in situ* bio-optical instruments, we obtained high-resolution information on P&P volume, type, and size at spatial scales significantly finer than if traditional methodologies had been applied. The improved sampling resolution from the automated methods led to greater spatial coverage and an increased size range of analysed P&P. Coupling the LISST and LOPC allowed us to observe a very wide P&P size spectra (3–5000 μm), which would be impossible with a single net and/or automatic counter. For mesozooplankton, the commonly used nets of 180–200 μm mesh size significantly underestimate small species and young developmental stages (Gallienne and Robins, 2001; Svendsen et al., 2011) and provide no data on aggregate concentrations, which are destroyed during straining. The approach of combining two instruments to simultaneously measure a wide range of P&P sizes contributed greatly to reducing the substantial gap in our knowledge about the P&P size structure and distribution in the vulnerable Arctic region. Another important advantage of such *in situ* size spectra measurements was the ability to track both spatial ecosystem variability and complementary hydrography.

4.2. Spatial variability of P&P structure

Environmental gradients along the water column enhance the patchy and layered distribution pattern of P&P (Dekshenieks et al., 2001; Möller et al., 2012; Trudnowska et al., 2016); in this study we observed a sharp decrease in P&P concentrations with depth (Fig. 4), which is a very common pattern in marine environments (e.g. Jackson and Checkley, 2011; Gluchowska et al., 2017). In our study, significant decrease in concentrations with depth was observed mainly in the case of phyto-, other- and snow-types of particles, which were concentrated in the upper 30/40 m. In general, the average size of P&P did not change along the water column. This was interesting, as we had expected to observe an increase in particle size with depth due to a kind of coagulation process caused by particles continuing to aggregate as they fall down, but probably some disaggregation processes were also going on (Burd and Jackson, 2009; Jackson & Checkley, 2011). Due to the high overall variability in the dataset, probably caused by the substantial P&P patchiness in this region (Trudnowska et al., 2016), and the uncertain origin of the observed P&P, we could not conclude if the different types and size fractions of P&P were vertically separated or matched as a result of mechanisms such as active feeding, niche portioning, or predator avoidance (Simon et al., 2002; Norrbin et al., 2009; Lalande et al., 2011).

Pronounced horizontal variability in zooplankton, protists, and particles has been observed in the Fram Strait region (Cherkasheva et al., 2014; Pavlov et al., 2015; Gluchowska et al., 2017). Spatial variability is equally important as environmental factors for zooplankton composition in this region (Weydmann et al., 2014). Coastal-offshore gradients in P&P structures have frequently been observed in many other locations worldwide (e.g. Hoproft et al., 2001; Mackas and Coyle, 2005; Buonassissi et al., 2010; Forest et al., 2012; Marcolin et al., 2013; Mackas et al., 2012; Garcia-Comas et al., 2014; Vandromme et al., 2014). These previous findings motivated us to compare the volume distribution and size structure of P&P in various sub-regions of the Fram Strait, but we did not observe a clear horizontal gradient (Fig. 6). This is likely due to the very complex and dynamic nature of the pathways of AW transport to the Arctic Ocean, which result in substantial mixing of both seawater and suspended P&P (Beszczynska-Möller et al., 2012; Trudnowska et al., 2016).

Nevertheless, we observed an interesting pattern: the concentration of phyto-type particles was pronounced in open waters (WSC and REC regions), while these particles were absent on the shelf stations (Fig. 5). This concurs with previous research showing that the processes occurring in the coastal zone around Svalbard suppress, rather than promote, phytoplankton growth (Cherkasheva et al., 2014). The phyto-type particles were larger in the WSC region (Fig. 4), implying that diatoms were present there, while the particles in the REC region were much smaller, potentially indicating phytoflagellate cells (Gluchowska et al., 2017). Phytoflagellate cells usually represent a majority of the phytoplankton abundance and biomass after the spring bloom in the polar seas (Not et al., 2005) and are expected to become a prevalent primary producer as global warming increases (Nöthig et al., 2015; Piwosz et al., 2015). We expected to observe a high contribution from large and transparent marine snow aggregates at the SS stations (Stramski et al., 2004; Marañón, 2015), due to the inflow of fresh waters containing terrigenous, mostly mineral material from fjords (Pavlov et al., 2015; Trudnowska et al., 2015) causing increased flocculation rates. However, the opposite result was found, which may be due to inappropriate fitting of the LOPC caused by considering the third mode of particles in the SS region (Supplementary Fig. 1) as zooplankton-type, following the method of Jackson & Checkley (2011). The generally observed trend that smaller marine snow aggregates contain more mineral particles, and the larger ones contain more organic matter, especially in regions dominated by algal particles (Jackson et al., 1997), most probably matched our observations in the Fram Strait, where larger volumes of marine snow aggregates were formed in productive open water locations and coastal waters were probably rather rich in mineral suspensions (Figs. 4 and 5).

The very large volumes of all types of P&P observed at the northern tip of the Svalbard coast and the western edges of the REC section (Fig. 6) could potentially be attributed to a few mechanisms. Firstly, particle flocculation may be enhanced by an inflow of fresh water (Zajączkowski, 2008, Meslard et al., 2018) from either the ice or the northern fjords (Figs. 1 and 5). Typically, ice edges and polynyas are areas of high productivity (Gradinger and Banmann, 1991) that attract large numbers of marine birds and mammals (Vacquié-Garcia et al., 2017). Upwelling and tidal mixing along the shelf-breaks of Svalbard could also substantially enhance the primary and secondary production through nutrient supply (Sakshaug, 2004; Falk-Petersen et al., 2015). In 2014, one year after the data collection for this study, high chlorophyll fluorescence was observed at almost the same time and in the same part of the northern Spitsbergen shelf (Granskog et al., 2015). While detritus and terrestrial particles are mainly transported locally, most organic components are advected via the WSC (Sanchez-Vidal et al., 2015). Advective transport of zooplankton organisms has been shown to be significant north of Svalbard (Daase et al., 2007; Blachowiak-Samolyk et al., 2008); it was recently estimated as 50 $kg{\cdot}C{\cdot}s^{-1}$ in August in the Fram Strait region (Basedow et al., 2018). Our study demonstrated that the core of surface warm water advection was much wider in northern regions, which closely corresponded with P&P accumulation patches (Fig. 7). This trend might be caused by the bathymetry of the area, as the main stream of the WSC flow is tightly confined to the Svalbard continental slope. However, as the shelf break significantly flattens in the northern part of the slope (Rudels et al., 2005), high velocity water recirculation as well as crossing the plateau (von Appen et al., 2016; Koenig et al., 2017) could result in the P&P advection inflow and accumulation area widening. Because the average concentration of P&P was similar among sections, the width of the transported mass may be important. A very high abundance of zooplankton in this area was observed previously (Kwasniewski et al., 2010; Trudnowska et al., 2012, 2015) and this region of Svalbard has been recognised as a rich feeding ground for higher trophic levels (Jakubas et al., 2013; Vacquié-Garcia et al., 2017). For the valued bowhead whales, the energy sources concentrated there are an important resource that might provide a road to recovery for their population (Falk-Petersen et al., 2015).

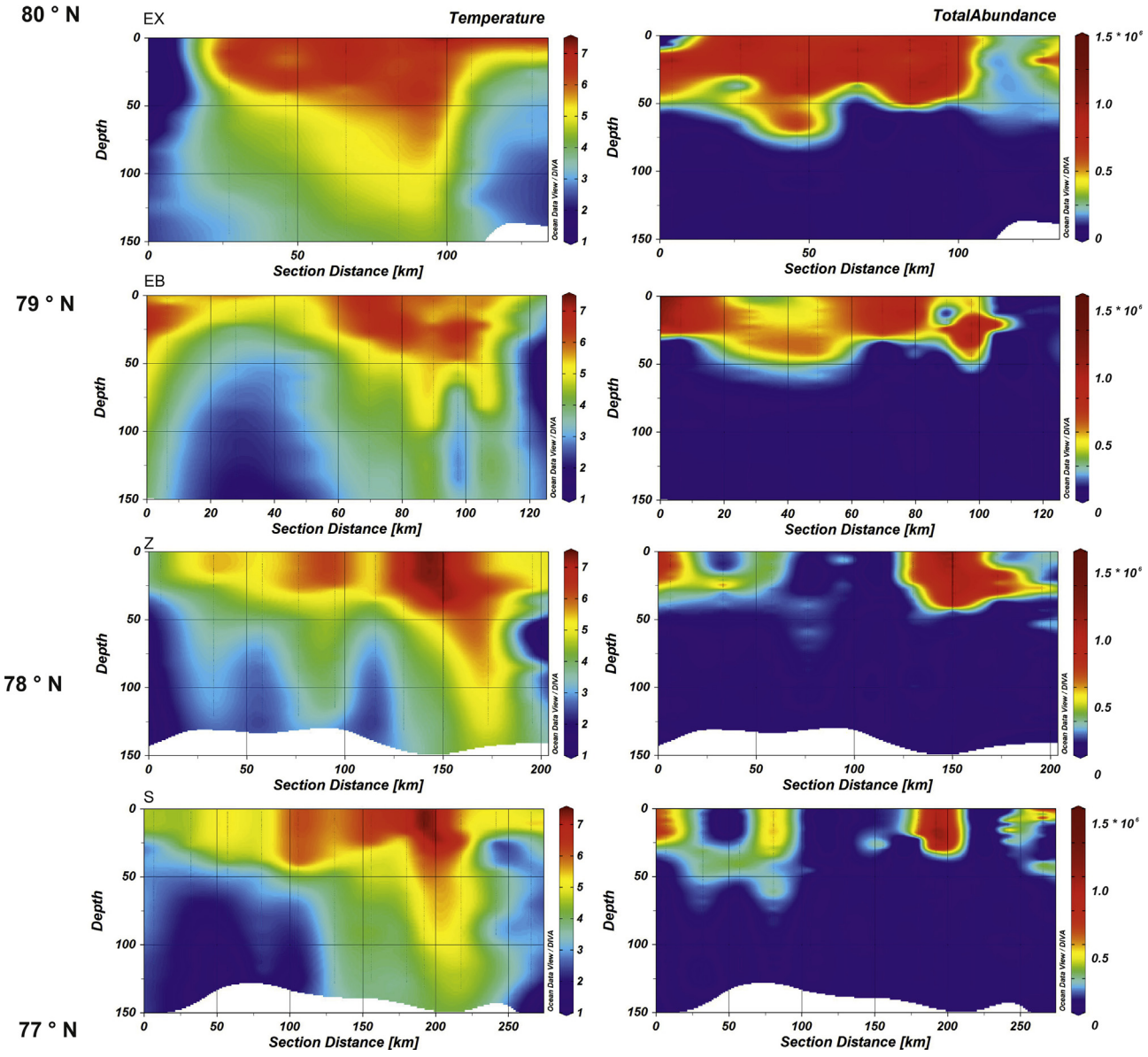

Fig. 7. The sections of temperature and total P&P abundance derived from high resolution LOPC measurements presents the width of the warm water and suspended matter advection at different latitudinal locations.

5. Conclusions

Our results indicate substantial spatial variability in P&P distribution, functional type, and size structure in the Fram Strait and show their coincidence with hydrodynamics, sea ice, and pelagic primary production. We identified a significantly rich biological hot spot in the shallower northern parts of the west Spitsbergen shelf, where the AW meets the ice edge. The coexistence of water masses with different physical and biological characteristics, as well as the presence of extensive sea ice and the Svalbard glacier melting processes, makes the Fram Strait region well suited for analysing the links between pelagic community structure and physical water properties in an era of climate change.

It remains unknown how climate change will affect the relationship between diverse size fractions and types of P&P in the warmer Arctic, but substantial modifications in ecological interactions and niche portioning are expected (Beaugrand et al., 2002; Mackas et al., 2007; Richardson, 2008; Beaugrand, 2009). The intensified glacier and river discharge results in more mineral and terrigenous particles entering the Arctic Ocean (Peterson et al., 2006), which enhances flocculation and aggregation processes. Moreover, the Arctic sea ice, which is one of the most rapidly changing components of the global climate system, is an extremely important factor for primary production (Arrigo et al., 2008). It affects the balance between stratification and mixing, fuelling the supply of new nutrients and forming a feeding ground for zooplankton and higher trophic levels.

Acknowledgments

This study was financed by Polish National Science Centre (PicMac project no. 2013/09/B/NZ8/03365) and Polish-Norwegian Research Programme under the Norwegian Financial Mechanism (DWARF project no. Pol-Nor/201992/93/2014). Additionally, S. Sagan was partially supported by the National Centre for Research and Development, Poland, under the Norwegian Financial Mechanism (2009–2014 Project CDOM-HEAT no. Pol-Nor/197511/40/2013). The language editing was financed by the funds of the Leading National Research Centre (KNOW) received by the Centre for Polar Studies for the period 2014-2018.

The authors want to acknowledge Marcin Wichorowski for his technical support as well as Jakub Kowalczyk for hard work and support during field measurements. The advice of Dr Agnieszka Beszczyńska-Moler on hydrographical sub-regions separation is also deeply appreciated by the authors. The authors are grateful to prof. Meng Zhou and Dr Sünnje Basedow for their substantial help at the beginning stage of the manuscript preparation. Special thanks are due to prof. George Jackson for his great help in providing the code for aggregate separation method from *nVd* spectrum.

Appendix A. Supplementary material

Supplementary data to this article can be found online at https://doi.org/10.1016/j.pocean.2018.09.005.

References

Agrawal, C., Pottsmith, H.C., 2000. Instruments for particle size and settling velocity observations in sediment transport. Mar. Geol. 168, 89–114.

Andrews, S.W., Nover, D.M., Reuter, J.E., Schladow, S.G., 2011. Limitations of laser diffraction for measuring fine particles in oligotrophic systems: pitfalls and potential solutions. Water Resour. Res. 47, W05523. https://doi.org/10.1029/2010WR009837.

Angles, S., Jordi, A., Garces, E., Maso, M., Basterretxea, G., 2008. High-resolution spatio-temporal distribution of a coastal phytoplankton bloom using laser in situ scattering and transmissometry (LISST). Harmful Algae 7, 808–816.

von Appen, W.-J., Schauer, U., Hattermann, T., Beszczynska-Möller, A., 2016. Seasonal cycle of mesoscale instability of the west Spitsbergen Current. J. Phys. Oceanogr. 46, 1231–1254.

Arrigo, K.R., Dijken, G. Van, Pabi, S., 2008. Impact of a shrinking Arctic ice cover on marine primary production. Arctic 35, 1–6.

Babin, M., Stramski, D., Ferrari, G.M., Claustre, H., Bricaud, A., Obolensky, G., Hoepffner, N., 2003. Variations in the light absorption coefficients of phytoplankton, nonalgal particles, and dissolved organic matter in coastal waters around Europe. J. Geophys. Res. 108, 3211.

Basedow, S.L., Tande, K.S., Norrbin, M.F., Kristiansen, S.A., 2013. Capturing quantitative zooplankton information in the sea : performance test of laser optical plankton counter and video plankton recorder in a *Calanus finmarchicus* dominated summer situation. North. Prog. Ocean. 108, 72–80.

Basedow, S.L., 2018. Seasonal variation in transport of Zooplankton into the Arctic basin through the Atlantic gateway. Front. Marine Sci. 5, 1–22.

Bauerfeind, E., Nöthig, E.M., Beszczynska, A., Fahl, K., Kaleschke, L., Kreker, K., Klages, M., Soltwedel, T., Lorenzen, C., Wegner, J., 2009. Particle sedimentation patterns in the eastern Fram Strait during 2000–2005: results from the Arctic long-term observatory HAUSGARTEN. Deep Sea Res I. 56, 1471–1487.

Bauerfeind, E., Nöthig, E.M., Pauls, B., Kraft, A., Beszczynska-Möller, A., 2014. Variability in pteropod sedimentation and corresponding aragonite flux at the Arctic deep-sea long-term observatory HAUSGARTEN in the eastern Fram Strait from 2000 to 2009. J. Mar. Syst. 132, 95–105.

Beaugrand, G., Luczak, C., Edwards, M., 2009. Rapid biogeographical plankton shifts in the North Atlantic Ocean. Glob. Change Biol. 15, 1790–1803.

Beaugrand, G., Reid, P.C., Ez, F., Lindley, J.A., Edwards, M., 2002. Reorganisation of North Atlantic marine copepod biodiversity and climate. Science 296, 692–1694.

Blachowiak-Samolyk, K., Kwasniewski, S., Dmoch, K., Hop, H., Falk-Petersen, S., 2007. Trophic structure of zooplankton in the Fram Strait in spring and autumn 2003. Deep Sea Res II 54, 2716–2728.

Blachowiaksamolyk, K., Soreide, J., Kwasniewski, S., Sundfjord, a, Hop, H., Falkpetersen, S., Nosthegseth, E., 2008. Hydrodynamic control of mesozooplankton abundance and biomass in northern Svalbard waters (79–81°N). Deep Sea Res. Part II. 55: 2210–2224.

Blanco, J.M., Echevarria, F., Garcia, C.M., 1994. Dealing with size-spectra: Some conceptual and mathematical problems. Scienta Marina. 58, 17–29.

Buonassissi, C.J., Dierssen, H.M., 2010. A regional comparison of particle size distributions and the power law approximation in oceanic and estuarine surface waters. J. Geophys. ResOceans 115, C10028.

Burd, A.B., Jackson, G.A., 2009. Particle aggregation. Ann. Rev. Mar. Sci. 1, 65–90.

Carmack, E.C., Yamamoto-Kawai, M., Haine, T.W.N., Bacon, S., Bluhm, B.A., Lique, C., Melling, H., Polyakov, I.V., Straneo, F., Timmermans, M.-L., et al., 2016. Freshwater and its role in the Arctic Marine System: Sources, disposition, storage, export, and physical and biogeochemical consequences in the Arctic and global oceans. J. Geophys. Res. Biogeosci. 121, 675–717. https://doi.org/10.1002/2015JG003140.

Carstensen, J., Weydmann, A., Olszewska, A., Kwaśniewski, S., 2012. Effects of environmental conditions on the biomass of Calanus spp. in the Nordic Seas. J. Plankton Res. 34, 951–966.

Cherkasheva, A., Bracher, A., Melsheimer, C., Köberle, C., Gerdes, R., Nöthig, E.M., Bauerfeind, E., Boetius, A., 2014. Influence of the physical environment on polar phytoplankton blooms: a case study in the Fram Strait. J. Mar. Syst. 132, 196–207.

Checkley, Jr, Davis, R.E., Herman, A.W., Jackson, G.A., Beanlands, B., Regier, L.A., 2008. Assessing plankton and other particles in situ with the SOLOPC. Limnol. Oceanogr. 53, 2123–2136.

Cisek, M., Colao, F., Demetrio, E., Di Cicco, A., Drozdowska, V., Fiorani, L., Goszczko, I., Lazic, V., Okladnikov, I.G., Palucci, A., Piechura, J., Poggi, C., Sighicelli, M., Walczowski, W., Wieczorek, P., 2010. Remote and local monitoring of dissolved and suspended fluorescent orqanic matter off Svalbard. J. Optoelectron. Adv. Mater. 12, 1604–1618.

Daase, M., Vik, J.O., Bagøien, E., Stenseth, N.C., Eiane, K., 2007. The influence of advection on Calanus near Svalbard: Statistical relations between salinity, temperature and copepod abundance. J. Plankton Res. 29, 903–911. https://doi.org/10.1093/plankt/fbm068.

Davies, E.J., Nimmo-Smith, W.A.M., Agrawal, Y.C., Souza, A.J., 2012. LISST-100 response to large particles. Mar. Geol. 307–310, 117–122. https://doi.org/10.1016/j.margeo.2012.03.006.

Dekshenieks, D.D., Donaghay, P.L., Sullivan, J.M., Rines, J.E.B., Osborn, T.R., Twardowski, M.S., 2001. Temporal and spatial occurrence of thin phytoplankton layers in relation to physical processes. Mar. Ecol. Prog. Ser. 223, 61–71.

Espinasse, B., Basedow, S., Schultes, S., Zhou, M., Berline, L., Carlotti, F., 2017. Conditions for assessing zooplankton abundance with LOPC in coastal waters. Prog. Oceanogr. 163, 260–270.

Falk-Petersen, S., Pavlov, V., Berge, J., Cottier, F., Kovacs, K.M., Lydersen, C., 2015. At the rainbow's end: high productivity fueled by winter upwelling along an Arctic shelf. Polar Biol. 38, 5–11.

Forest, A., Stemmann, L., Picherall, M., Burdorf, L., Robert, D., Fortier, L., Babin, M., 2012. Size distribution of particles and zooplankton across the shelf-basin system in southeast Beaufort Sea: combined results from an Underwater Vision Profiler and vertical net tows. Biogeosciences 9, 1301–1320.

Gallienne, C.P., Robins, D.B., 2001. Is *Oithona* the most important copepod in the world's oceans? J. Plankton Res. 23, 1421–1432.

García-Comas, C.C.Y., Chang, L., Ye, A.R., Sastri, Y.C., Lee, G.C. Gong, Hsieh, C.H., 2014. Mesozooplankton size structure in response to environmental conditions in the East China Sea: How much does size spectra theory fit empirical data of a dynamic coastal area? Prog. Oceanogr. 121, 141–157.

Gluchowska, M., Trudnowska, E., Goszczko, I., Kubiszyn, A., Blachowiak-Samolyk, K., Walczowski, W., Kwasniewski, S., 2017. Variations in the structural and functional diversity of zooplankton over vertical and horizontal gradients en route to the Arctic Ocean through the Fram Strait. Plos One 12 (2), e0171715.

González-Quirós, R., Checkley, D.M., 2006. Occurrence of fragile particles inferred from optical plankton counters used in situ and to analyze net samples collected simultaneously. J. Geophys. Res. 111, 1–12.

Gradinger, R.R., Banmann, M.E.M., 1991. Distribution of phytoplankton communities in relation to the large-scale hydrographical regime in the Fram Strait. East 321, 311–321.

Graham, G.W., Davies, E.J., Nimmo-Smith, W.a.M., Bowers, D.G., Braithwaite, K.M., 2012. Interpreting LISST-100X measurements of particles with complex shape using digital in-line holography. J. Geophys. Res. Oceans 117.

Granskog, M.A., Pavlov, A.K., Sagan, S., Raczkowska, A., Stedmon, 2015. Effect of sea-icemelt on inherent optical properties and vertical distribution of solar radiant heating in Arctic surface waters. J. Geophys. Res. Ocean. 1–16.

Herman, A.W., 1992. Design and calibration of a new optical plankton counter capable of sizing small zooplankton. Deep-Sea Res. A 39, 395–415.

Herman, A.W., Beanlands, B., Phillips, E.F., 2004. The next generation of Optical Plankton Counter: The Laser-OPC. J. Plankton Res. 26, 1135–1145.

Hop, H., Falk-Petersen, S., Svendsen, H., Kwasniewski, S., Pavlov, V., Pavlova, O., Søreide, J.E., 2007. Physical and biological characteristics of the pelagic system across Fram Strait to Kongsfjorden. Prog. Oceanogr. 71, 182–231.

Hopcroft, R., Roff, J., Chavez, F., 2001. Size paradigms in copepod communities: a re-examination. Hydrobiologia 453, 133–141.

Jackson, G.A., Maffione, R., Costello, D.K., Alldredge, A.L., Logan, B.E., Dam, H.G., 1997. Particle size spectra between 1 μm and 1 cm at Monterey Bay determined using multiple instruments. Deep Sea Res. I. 44, 1739–1767.

Jackson, G.A., Checkley Jr., D.M., 2011. Particle size distributions in the upper 100 m water column and their implications for animal feeding in the plankton. Deep Sea Res I 58, 283–297.

Jackson, G.A., Checkley, D.M., Dagg, M., 2015. Settling of particles in the upper 100m of the ocean detected with autonomous profiling floats off California. Deep. Res. I 99, 75–86.

Jakubas, D., Trudnowska, E., Wojczulanis-Jakubas, K., Iliszko, L., Kidawa, D., Darecki, M., Blachowiak Samolyk, K., Stempniewicz, L., 2013. Foraging closer to the colony leads to faster growth in little auks. Mar. Ecol. Prog. Ser. 489, 263–278.

Jennings, S., Warr, K.J., Mackinson, S., 2002. Use of size-based production and stable isotope analyses to predict trophic transfer efficiencies and predator-prey body mass ratios in food webs. Mar. Ecol. Prog. Ser. 240, 11–20.

Karp-Boss, L., Azevedo, L., Boss, E., 2007. LISST-100 measurements of phytoplankton size distribution: evaluation of the effects of cell shape. Limnol. Oceanogr: Methods 5, 396–406.

Kerr, S.R., Dickie, L.M., 2001. The Biomass Spectrum: A Predator-prey Theory of Aquatic Production. Columbia University Press, New York.

Koenig, Z., Provost, C., Villacieros-Robineau, N., Sennéchael, N., Meyer, A., Lellouche, J.M., Garric, G., 2017. Atlantic waters inflow north of Svalbard: Insights from IAOOS observations and Mercator Ocean global operational system during N-ICE2015. J. Geophys. Res. Ocean. 122, 1254–1273. https://doi.org/10.1002/2016JC012424.

Kraft, A., Bauerfeind, E., Nöthig, E.M., Bathmann, U.V., 2012. Size structure and life cycle patterns of dominant pelagic amphipods collected as swimmers in sediment traps in the eastern Fram Strait. J. Mar. Syst. 95, 1–15.

Krupica, K.L., Sprules, W.G., Herman, A.W., 2012. The utility of body size indices derived from optical plankton counter data for the characterization of marine zooplankton assemblages. Cont. Shelf Res. 36, 29–40.

Kwasniewski, S., Gluchowska, M., Jakubas, D., Walkusz, W., Karnovsky, N., 2010. The impact of different hydrographic conditions and zooplankton communities on provisioning Little Auks along the West coast of Spitsbergen. Prog. Oceanogr. 87, 72–82.
Lalande, C., Bauerfeind, E., Nöthig, E.M., 2011. Downward particulate organic carbon export at high temporal resolution in the eastern Fram Strait: influence of Atlantic Water on flux composition. Mar. Ecol. Prog. Ser. 440, 127–136.
Lane, P.V.Z., Llinăs, L., Smith, S.L., Pilz, D., 2008. Zooplankton distribution in the western Arctic during summer 2002: hydrographic habitats and implications for food chain dynamics. J. Mar. Syst. 70, 97–133.
Mackas, D.L., Batten, S., Trudel, M., 2007. Effects on zooplankton of a warmer ocean: recent evidence from the Northeast Pacific. Prog. Oceanogr. 75, 223–252.
Mackas, D.L., Coyle, K.O., 2005. Shelf-offshore exchange processes, and their effects on mesozooplankton biomass and community composition patterns in the northeast Pacific. Deep Sea Res. II. 52, 707–725.
Mackas, D.L., Pepin, P., Verheye, H., 2012. Interannual variability of marine zooplankton and their environments: within- and between-region comparisons. Prog. Oceanogr. 97–100, 1–14.
Marañón, E., 2015. Cell size as a key determinant of phytoplankton metabolism and community structure. Ann. Rev. Mar. Sci. 7, 241–264. https://doi.org/10.1146/annurev-marine-010814-015955.
Marcolin, C., Schultes, S., Jackson, G.A., Lopes, R.M., 2013. Plankton and seston size spectra estimated by the LOPC and ZooScan in the Abrolhos Bank ecosystem (SE Atlantic). Cont. Shelf Res. 70, 74–87.
Meslard, F., Bourrin, F., Many, G., Kerhervé, P., 2018. Suspended particle dynamics and fluxes in an Arctic fjord (Kongsfjorden, Svalbard). Estuar. Coast. Shelf Sci. 204, 212–224.
Mikkelsen, O.A., Hill, P.S., Milligan, T.G., Chant, R.J., 2005. In situ particle size distributions and volume concentrations from a LISST-100 laser particle sizer and a digital floc camera. Cont. Shelf Res. 25, 1959–1978.
Möller, K.O., St, M., John, A., Temming, J., Floeter, A.F., Sell, J.-P. Herrmann, Möllmann, C., 2012. Marine snow, zooplankton and thin layers: indications of a trophic link from small-scale sampling with the Video Plankton Recorder. Mar. Ecol. Prog. Ser. 468, 57–69.
Nagelkerke, N.J.D., 1991. A note on a general definition of the coefficient of determination. Biometrika 78, 691–692.
Norrbin, F., Eilertsen, H.C., Degerlund, M., 2009. Vertical distribution of primary producers and zooplankton grazers during different phases of the Arctic spring bloom. Deep Sea Res II. 56, 1945–1958.
Not, F., Massana, R., Latasa, M., Marie, D., Colson, C., Eikrem, W., Pedros Alio, C., Vaulot, D., Simon, N., 2005. Late summer community composition and abundance of photosynthetic picoeukaryotes in Norwegian and Barents Seas. Limnol. Oceanogr. 50, 1677–1686.
Nöthig, E.M., Bracher, A., Engel, A., Metfies, K., Niehoff, B., Peeken, I., Bauerfeind, E., Cherkasheva, A., Gäbler-Schwarz, S., Hardge, K., Kilias, E., Kraft, A., Kidane, Y.M., Lalande, C., Piontek, J., Thomisch, K., Wurst, M., 2015. Summertime plankton ecology in Fram Strait – a compilation of long- and short-term observations. Polar Res. 34, 23349.
Pasternak, A., Arashkevich, E., Reigstad, M., Wassmann, P., Falk-Petersen, S., 2008. Dividing mesozooplankton into upper and lower size groups: applications to the grazing impact in the Marginal Ice Zone of the Barents Sea. Deep Sea Res II. 55, 2245–2256.
Pavlov, A.K., Granskog, M.A., Stedmon, C.A., Ivanov, B.V., Hudson, S.R., Falk-Petersen, S., 2015. Contrasting optical properties of surface waters across the Fram Strait and its potential biological implications. J. Mar. Syst. 143, 62–72.
Peterson, B.J., Mcclelland, J., Curry, R., Holmes, R.M., Walsh, J.E., Aagaard, K., 2006. Trajectory shifts in the Arctic and Subarctic Freshwater Cycle. Science 313, 1061–1066.
Petrik, C.M., Jackson, G.A., Checkley, Jr, 2013. Aggregates and their distributions determined from LOPC observations made using an autonomous profiling float. Deep Sea Res. Part I : Oceanogr. Res. Pap. 74, 64–81.
Piechura, J., Beszczyńska-Möller, A., Osinski, R., 2001. Volume, heat and salt transport by the West Spitsbergen Current. Polar Res. 20, 233–240.
Piwosz, K., Spich, K., Całkiewicz, J., Weydmann, A., Kubiszyn, A.M., Wiktor, J.M., 2015. Distribution of small phytoflagellates along an Arctic fjord transect. Environ. Microbiol. 17, 2393–2406.
Quéré, C.L., Harrison, S.P., Colin Prentice, I., Buitenhuis, E.T., Aumont, O., Bopp, L., Claustre, H., Cotrim Da Cunha, L., Geider, R., Giraud, X., Klaas, C., Kohfeld, K.E., Legendre, L., Manizza, M., Platt, T., Rivkin, R.B., Sathyendranath, S., Uitz, J., Watson, A.J., Wolf-Gladrow, D., 2005. Ecosystem dynamics based on plankton functional types for global ocean biogeochemistry models. Glob. Change Biol. 11, 2016–2040.
Reynolds, R.A., Stramski, D., Wright, V.M., Woźniak, S.B., 2010. Measurements and characterization of particle size distributions in coastal waters. J. Geophys. Res. Oceans, 115.
Richardson, A.J., 2008. In hot water: zooplankton and climate change. ICES J. Mar. Sci. 65, 279–295.
Richardson, A.J., Schoeman, D.S., 2004. Climate impact on Plankton ecosystems in the Northeast Atlantic. Science 305, 1609–1612.
Rudels, B., Björk, G., Nilsson, J., Winsor, P., Lake, I., Nohr, C., 2005. The interaction between waters from the Arctic Ocean and the Nordic Seas north of Fram Strait and along the East Greenland current: results from the Arctic Ocean-02 Oden expedition. J. Mar. Syst. 55, 1–30.
Saiz, E., Calbet, A., Isari, S., Antó, M., Velasco, E.M., Almeda, R., Movilla, J., Alcarez, M., 2013. Zooplankton distribution and feeding in the Arctic Ocean during a Phaeocystis pouchetii bloom. Deep Sea Res I. 72, 17–33.
Sakshaug, E., 2004. Primary and Secondary Production in the Arctic Seas. In: Stein, R., MacDonald, R. (Eds.), The Organic Carbon Cycle in the Arctic Ocean. Springer, Berlin Heidelberg, pp. 57–81.
Saloranta, T.M., Haugan, P.M., 2004. Northward cooling and freshening of the warm core of the West Spitsbergen Current. Polar Res. 23, 79–88.
Sanchez-Vidal, A., Veres, O., Langone, L., Ferré, B., Calafat, A., Canals, M., Durrieu de Madron, X., Heussner, S., Mienert, J., Grimalt, J.O., Pusceddu, A., Danovaro, R., 2015. Particle sources and downward fluxes in the eastern Fram Strait under the influence of the west Spitsbergen Current. Deep Res. Part I Oceanogr. Res. Pap. 103, 49–63.
Schauer, U., Fahrbach, E., Osterhus, S., Rohardt, G., 2004. Arctic warming through the Fram Strait: Oceanic heat transport from 3 years of measurements. J. Geophys. Res. 109, C06026.
Schlitzer, R., 2015. Ocean Data View, http://odv.awi.de.
Schlichtholz, P., Houssais, M.N., 2002. An overview of the θ–S correlations in Fram Strait based on the MIZEX 84 data. Oceanologia 44, 243–272.
Serra, T., Colomer, J., Soler, M., Vila, X., 2003. Spatio-temporal heterogeneity in a planktonic Thiocystis minor population, studied by laser in situ particle analysis. Freshw. Biol. 48, 698–708.
Simon, M., Grossart, H.-P., Schweitzer, B., Ploug, H., 2002. Microbial ecology of organic aggregates in aquatic ecosystems. Aquat. Microb. Ecol. 2, 175–211.
Sprules, W.G., Barth, L.E., 2015. Surfing the biomass size spectrum: some remarks on history, theory, and application. Can. J. Fish. Aquat. Sci. 73, 477–495.
Stemmann, L., Picheral, M., Guidi, L., Lombard, F., Prejger, F., Claustre, H., Gorsky, G., 2008. Assessing the spatial and temporal distributions of zooplankton and marine particles using the Underwater Vision Profiler. Biogoesciences 5, 299–310.
Stramski, D., Boss, E., Bogucki, D., Voss, K.J., 2004. The role of seawater constituents in light backscattering in the ocean. Prog. Oceanogr. 61, 27–56.
Svendsen, C., Seuthe, L., Vasilyeva, Y., Pasternak, A., Hansen, E., 2011. Zooplankton distribution across Fram Strait in autumn: Are small copepods and protozooplankton important? Prog. Oceanogr. 91, 534–544.
Trudnowska, E., Basedow, S.L., Blachowiak-Samolyk, K., 2014. Mid-summer mesozooplankton biomass, its size distribution, and estimated production within a glacial Arctic fjord (Hornsund, Svalbard). J. Mar. Syst. 137, 55–66.
Trudnowska, E., Sagan, S., Kwasniewski, S., Darecki, M., Blachowiak-Samolyk, K., 2015. Fine-scale zooplankton vertical distribution in relation to hydrographic and optical characteristics of the surface waters on the Arctic shelf. J. Plankton Res. 37, 120–133.
Trudnowska, E., Szczucka, J., Hoppe, L., Boehnke, R., Hop, H., Blachowiak-Samolyk, K., 2012. Multidimensional zooplankton observations on the northern West Spitsbergen Shelf. J. Mar. Syst. 98–99, 18–25.
Trudnowska, E., Gluchowska, M., Beszczynska-Möller, A., Blachowiak-Samolyk, K., Kwasniewski, S., 2016. Plankton patchiness in the Polar Front region of the West Spitsbergen Shelf. Mar. Ecol. Prog. Ser. 560, 1–18.
Vacquié-Garcia, J., Lydersen, C., Marques, T.A., Aars, J., Ahonen, H., Skern-Mauritzen, M., Øien, N., Kovacs, K.M., 2017. Late summer distribution and abundance of ice-associated whales in the Norwegian High Arctic. Endangered Spec. Res. 32, 59–70.
Vandromme, P., Nogueira, E., Huret, M., Lopez-Urrutia, A., González-Nuevo González, G., Sourisseau, M., Petitgas, P., 2014. Springtime zooplankton size structure over the continental shelf of the Bay of Biscay. Ocean Sci. 10, 821–835.
Walczowski, W., 2013. Frontal structures in the West Spitsbergen Current margins. Ocean Sci. 9, 957–975.
Wassmann, P.M., Reigstad, T., Haug, B. Rudels, Carroll, M.L., Hop, H., Wing Gabrielsen, G., Falk-Petersen, S., Denisenko, S.G., Arashkevich, E., Slagstad, D., Pavlov, O., 2006. Food webs and carbon flux in the Barents Sea. Prog. Oceanogr. 71, 232–287.
Wekerle, C., Wang, Q., von Appen, W.-J., Danilov, S., Schourup-Kristensen, V., Jung, T., 2017. Eddy-resolving simulation of the Atlantic Water circulation in the Fram Strait with focus on the seasonal cycle. J. Geophys. Res. Oceans. https://doi.org/10.1002/2017JC012974.
Weydmann, A., Carstensen, J., Goszczko, I., Dmoch, K., Olszewska, A., Kwasniewski, S., 2014. Shift towards the dominance of boreal species in the Arctic: inter-annual and spatial zooplankton variability in the West Spitsbergen Current. Mar. Ecol. Prog. Ser. 501, 41–52.
Wiebe, P.H., Benfield, M.C., 2003. From the Hensen net toward four-dimensional biological oceanography. Prog. Oceanogr. 56, 7–136.
Worden, A.Z., Follows, M.J., Giovannoni, S.J., Wilken, S., Zimmerman, A.E., Keeling, P.J., 2015. Rethinking the marine carbon cycle: Factoring in the multifarious lifestyles of microbes. Science 347, 6223.
Zajączkowski, M., 2008. Sediment supply and fluxes in glacial and outwash fjords. Kongsfjorden and Adventfjorden, Svalbard 29, 59–72.